Experimental Heat Transfer
Publication details, including instructions for authors and subscription information:
http://www.informaworld.com/smpp/title~content=t713770473

MEASUREMENT OF INFRARED ABSORPTION COEFFICIENTS OF MOLTEN GLASSES

Zhaoyan Zhang ; Michael F. Modest ;Sudarshan P. Bharadwaj

To cite this Article Zhang, Zhaoyan , Modest, Michael F. andBharadwaj, Sudarshan P.(2001) 'MEASUREMENT OF INFRARED ABSORPTION COEFFICIENTS OF MOLTEN GLASSES', Experimental Heat Transfer, 14: 3, 145 — 156
To link to this Article: DOI: 10.1080/08916150120017
URL: http://dx.doi.org/10.1080/08916150120017

Experimental Heat Transfer, 14:145–156, 2001

0891-6152/01 $12.00 + .00

MEASUREMENT OF INFRARED ABSORPTION COEFFICIENTS OF MOLTEN GLASSES

Zhaoyan Zhang
Department of Mechanical Engineering—Engineering Mechanics, Michigan Technological University, Houghton, Michigan, USA

Michael F. Modest and Sudarshan P. Bharadwaj
Department of Mechanical Engineering, The Pennsylvania State University, University Park, Pennsylvania, USA

In this article, a method based on the "submerged mirror" technique to measure the absorption coefficient of molten glass is presented. Infrared light, which is modulated by Michelson's interferometeric setup, passes through the molten glass and is collected by a mercury-cadmium-telluride (MCT) or a silicon detector. The signal is processed by a Fourier transform infrared (FTIR) spectrometer to yield the spectral intensity of the infrared light. The processes are repeated with different thicknesses of molten glass layer. The spectral absorption coefficient is calculated from the apparent transmittance. Tests of the apparatus have been made with distilled water, for which the results agree well with existing data. Measurements were carried out for a number of calcia-alumina-silicate glasses at temperatures ranging from 1,200 to 1,300°C.

Radiative heat transfer is an important—if not the most dominant—mode of heat transfer during the drawing of E-glass through bushings. For optimal control of the fiber drawing process, the radiative heat losses must be accurately determined and/or tailored, which requires detailed and accurate knowledge of the glass's absorption coefficient at high temperature.

Methods to measure optical properties of liquids can be broadly classified into emission techniques [1, 2], acousto-optics [3], ellipsometry [4, 5], Kramers-Kronig transforms [6, 7], pole-fit procedures [8], transmission techniques [9–13], and submerged-mirror techniques [14, 15].

An error analysis using representative errors in emissivity measurements shows that emission techniques are very sensitive to temperature measurement errors. The use of acousto-optics requires microphones that can withstand temperatures greater than 1,000°C, which have not been developed yet. The performance-to-cost ratio of setups in ellipsometric methods justify their use only for high-accuracy measurements of the complex index of refraction. Kramers-Kronig transforms need measurements over a wide spectral range to achieve reasonable accuracy. Mackenzie [10] and Greenberg [9] have performed transmission measurements by holding a thin film of liquid with platinum

Financial support for this work by Owens Corning, Inc., is gratefully acknowledged.

Address correspondence to Zhaoyan Zhang, Department of Mechanical Engineering—Engineering Mechanics, 815 R. L. Smith ME-EM Building, Houghton, MI 49931-1295, USA.

NOMENCLATURE

A	surface area	κ	absorption coefficient
d	glass layer thickness	ρ	reflectance
E	sample emission spectrum	τ	transmittance
$I_{b\eta}$	spectral blackbody radiation intensity at wavenumber η	**Subscripts**	
P	quantity that is proportional to blackbody radiation intensity	b	blackbody
		g	glass
P_η	radiation intensity at wavenumber η	m	mirror
R	measured IR spectrum	i	image
S	true transmission spectrum	s	source
T	temperature	sa	sample
ϵ	emittance	so	source
θ	solid angle	η	wavenumber

loops and meshes. Others have made measurements using custom-made cells with sapphire or MgO windows [13]. For the present investigation, commercial liquid cells cannot be used, as they cannot withstand high temperatures. Therefore, for the measurement of absorption coefficients of liquid glasses, submerged-mirror techniques appear to be the most suitable.

This technique was first proposed by Ebert and Self [14]. It was later adopted by Gupta and Modest [15] to measure the absorption coefficient of LiF and LiS_2. In the present study, an improved setup has been constructed to measure the absorption coefficient of molten glass. This setup incorporates a Fourier transform infrared (FTIR) spectrometer, which filters out unmodulated background radiation and measures a wide range of spectral intensity in one operation. A platinum crucible is mounted on an alumina tube which can be adjusted vertically with micrometer precision.

EXPERIMENTAL SETUP

Figure 1 is a schematic of the setup. The centerpiece of this setup is an FTIR spectrometer (Mattson Galaxy). The FTIR has a tungsten near-infrared source operating at 3,000 K. The tungsten filament is enclosed in a quartz envelope, which blocks any infrared radiation beyond the wavelength of roughly 5 μm. The infrared beam is modulated by a Michelson's interferometric setup. It is then passed through an optical path and is picked up by a detector. The detector can be either a mercury-cadmium-telluride (MCT) detector or a silicon detector, each working over a different wavelength range. The resulting interferogram contains the spectral information of the infrared beam. A software package accompanying the FTIR performs a Fourier transform to convert the interferogram to spectral data.

The optical path consists of five flat mirrors (F1, F2, F3, F4, and F5), two spherical mirrors (S1 and S2), two irises (I1 and I2), and two lenses (a zinc selenide lens and a normal glass lens). Mirrors F1, F3, F4, F5, S1, and S2 are made of protected gold and were purchased from Edmund Scientific. Each of the mirrors (F1, F3, F4, F5, S1, and S2) is mounted on a kinematic mirror mount so that its orientation can be fine-adjusted. Mirror F2 is a polished platinum disk and was provided by Owens Corning. Inspection

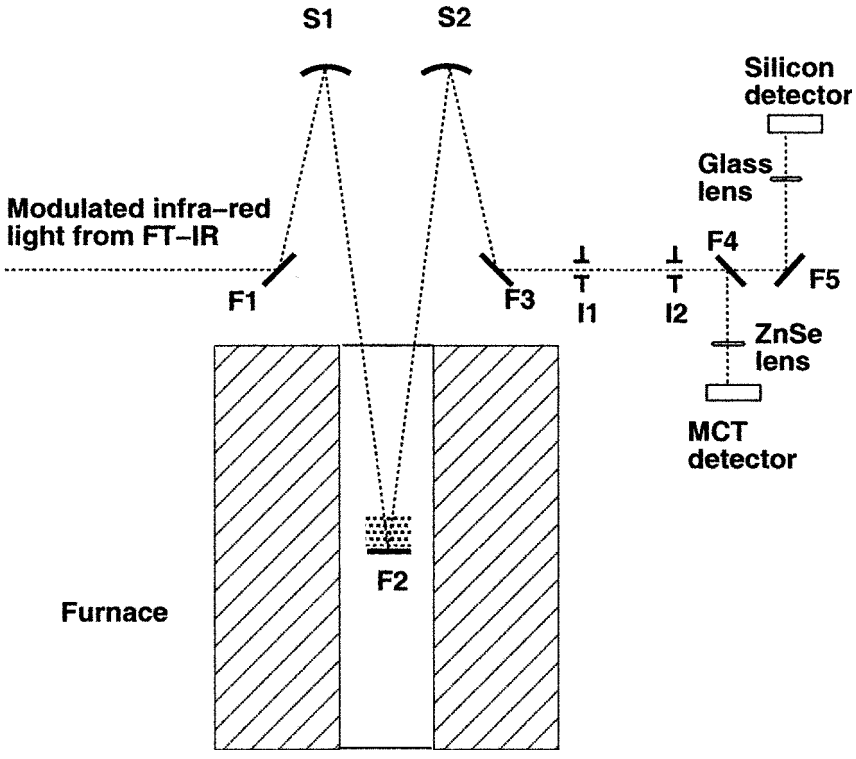

Figure 1. Schematic of experimental setup.

of the polished platinum disk using visible light indicates that the polished disk can be considered fully specular. The platinum mirror is placed on a platinum mirror holder and is submerged in the molten glass. The mirror holder is suspended by three platinum rods, which can be adjusted to facilitate the alignment of the optical path. Because the molten glass is of high viscosity even at over 1,000°C, submerging the platinum mirror into molten glass may cause lateral movement of the mirror and disturb the optical alignment. Three set screws are used to secure the platinum rods after the optical adjustment has been done. The crucible is placed on top of an alumina pedestal, which is attached to a linear translation stage. The thickness of the glass layer is adjusted by raising the crucible, and thus the glass level, while keeping the platinum mirror stationary.

The infrared beam coming from the FTIR opening first hits mirror F1 and is reflected to spherical mirror S1, which is of 18-in. focal length. The spherical mirror forms an image on the flat mirror F2. This image is then re-imaged by mirror S2 (12-in. focal length) to project an image through mirror F3 at iris I2. Thus the iris I2 is used as a field stop to cut down the size of the source being seen by the detector. The infrared light leaving the iris I2 is reflected by one of the two flat mirrors (F4 or F5) and is directed to either a silicon detector or a MCT detector. The light beam passes through a lens and is focused onto the detectors. The detectors are placed on separate translation stages to allow fine adjustment of their position. Iris I1 is placed along the optical path to allow the adjustment of solid angle of the source beam and, thus, adjust the energy that hits the

detectors. The optical alignment is first made for the silicon detector at the back. The flat mirror F4 is then inserted into the optical path to direct the infrared beam to the MCT detector in the front. When conducting experiments, the measurements with the MCT detector are carried out first. The flat mirror F4 is removed after the measurements using the MCT detector, and the experiments with the silicon detector can then be conducted.

EXPERIMENTAL PROCEDURE

When a beam is incident normal to the surface of molten glass, multiple reflections will occur. If the submerged mirror is not parallel to the glass surface, it is possible to separate the multiple reflections from another as shown in Figure 2. In our case, the second reflection is separated from the rest and is sent to the detector. The strength of the spectral IR radiation reaching the detector at wavenumber η can be expressed as

$$P_\eta = A_s \epsilon_s \theta_s I_{b\eta} (1 - \rho_{12})^2 \rho_{23} \tau_\eta^2; \tag{1}$$

where A_s is the area of the source, θ_s is the solid angle of the source, ϵ_s is the emittance, $I_{b\eta}$ is the spectral blackbody radiation within the spectral range of the detector, ρ_{12} is the reflectivity of the glass–air interface, ρ_{23} is the reflectivity of the platinum glass interface, and $\tau_\eta = \exp(-\kappa_\eta d)$ is the transmittance for glass layer thickness d. If $P_{\eta 1}$ and $P_{\eta 2}$ are the radiation intensities reaching the detector for glass layer thicknesses d_1 and d_2, respectively, one can express the absorption coefficient as

$$\kappa_\eta = -\frac{1}{2(d_1 - d_2)} \ln \frac{P_{\eta 1}}{P_{\eta 2}} \tag{2}$$

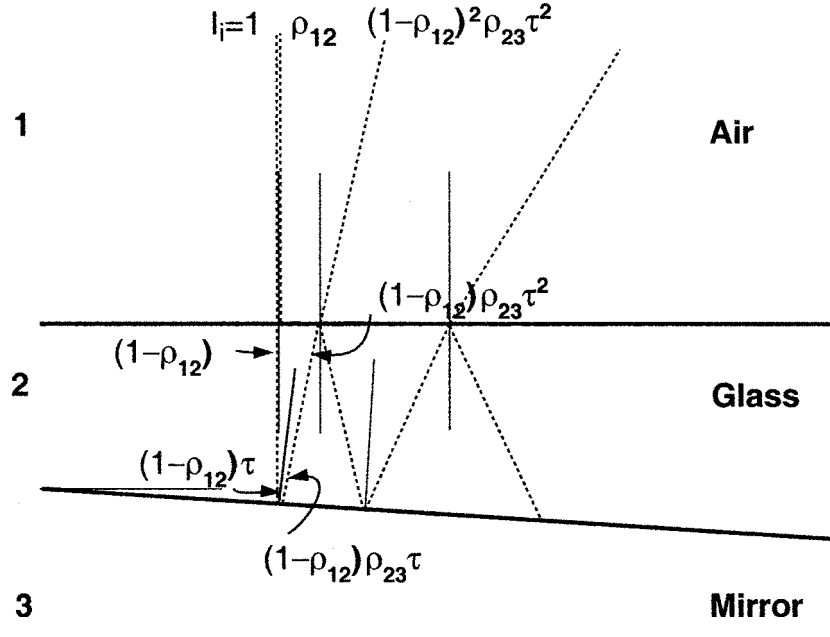

Figure 2. Reflectivity and transmittance of a thick transparent slab.

Thus $\kappa(\eta; T)$ can be determined if $P_{\eta 1}$ and $P_{\eta 2}$ and $(d_1 - d_2)$ are known. The outputs $P_{\eta 1}$ and $P_{\eta 2}$ are measured by the FTIR. The thickness difference $(d_1 - d_2)$ is determined from the translation stage that raises the crucible (adjusted for the changing volume of the immersed portion of the mirror support rods).

In the current study, we are interested in the absorption coefficient of glass at elevated temperatures. It has been shown that the introduction of a hot sample into the optical path will cause severe error in deriving spectral properties from the measurements of transmittance [16]: not only emission from all components in the source compartment is modulated and contributes to the interferogram, but the emission originating from the optics and hot test sample will be imaged into the Michelson's interferometric setup, modulated, and subsequently imaged back onto the detector. Fringes generated by the radiation, which is reflected back into the interferometric setup, are π radians out of phase with those generated by the radiation from the internal source. The measured interferogram contains contributions from all emitting sources. However, practically, only the emission from the source and the hot sample are of appreciable strength and of concern.

For the experimental arrangement shown in Figure 3, neglecting the small reflectance of the glass–air interface for this qualitative assessment, the modulated infrared radiation reaching the detector can be expressed as

$$R = S - E = (1 - \epsilon_m)\tau^2 P_s - (1 - \epsilon_m)\epsilon_m \tau^3 P_m - (1 - \tau)\tau^2 P_g \tag{3}$$

where R is the measured spectrum, S is the true transmission spectrum, E is the sample emission spectrum, ϵ_m is the emittance of the mirror, τ is the transmittance of the glass

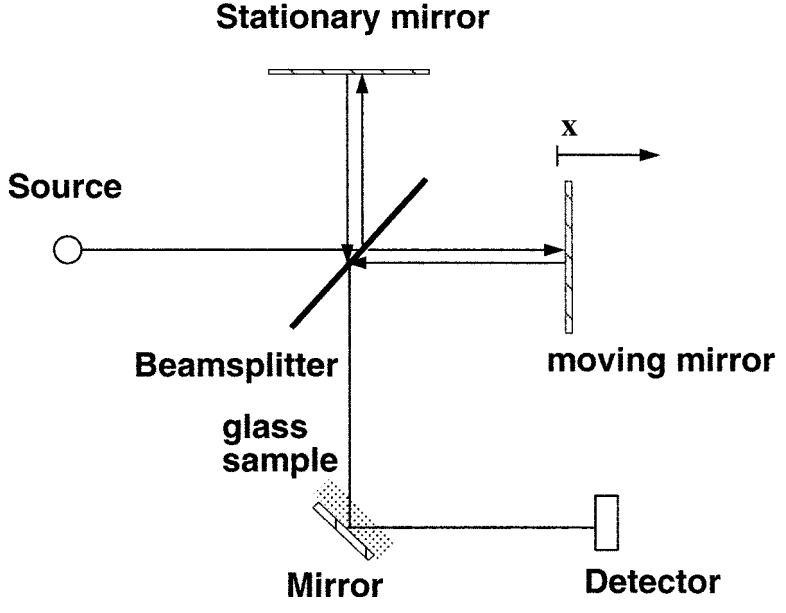

Figure 3. Schematic of a interferometric setup intended to measure the transmittance using submerged-mirror technique.

layer, P_s is proportional to blackbody radiation from the source, P_m is proportional to blackbody radiation from the mirror, and P_g is proportional to blackbody radiation from the glass layer and is equal to P_m. Assuming the source operates at 2,700°C and the mirror and sample are at 1,300°C, the emitted signal from the mirror and sample can reach the same order of magnitude as the transmitted signal from the source. Ratioing the signals taken with different glass layer thicknesses results in

$$\text{ratio} = \frac{\tau^2(d_1)}{\tau^2(d_2)} \times \frac{(1-\epsilon_m)P_s - (1-\epsilon_m)\epsilon_m\tau(d_1)P_m - (1-\tau(d_1))P_g}{(1-\epsilon_m)P_s - (1-\epsilon_m)\epsilon_m\tau(d_2)P_m - (1-\tau(d_2))P_g} \tag{4}$$

Since the second term on the right-hand side is not unity, this ratio is not directly proportional to the transmittance of the glass layer. A number of measures have been proposed to correct this problem [16, 17]. These include (1) modification of the interferometer such that the emission from the sample is not imaged onto the detector; (2) chopping of the source radiation and demodulation of the signal using a lock-in amplifier; (3) use of two sources, each operating at a different temperature. Subtracting the two signals will cancel the sample emission.

In our experiments, the effects of sample emission were corrected by the so-called partially blocked beam method [18], taking advantage of the corner-cube optics used in the Mattson FTIR spectrometer. The emission from the sample reexiting such a spectrometer after modulation is offset with respect to the incoming unmodulated emission. By blocking half the aperture of the FTIR compartment, the emission from the sample enters the spectrometer and is modulated, but is blocked from exiting the FTIR on its way to the detector. Thus, the signal measured with half the aperture of the FTIR compartment blocked gives a true transmission spectrum. We then have

$$P = (1-\epsilon_m)\tau^2 P_s \tag{5}$$

and the spectral absorption coefficients can be derived by applying Eq. (2) directly.

It was found that the AC preamplifier of the detector malfunctions when the detector is subject to too strong unmodulated radiation. Thus, it is of advantage to suppress the part of the sample emission that hits the detector which falls outside the solid angle of the source emission, while maintaining maximum source radiation that hits the detector. The ratio of the modulated emissive power from the source seen by the detector P_{so} versus the unmodulated emissive power of the sample seen by the detector P_{sa} can be expressed as

$$\frac{P_{\text{so}}}{P_{\text{sa}}} = \frac{A_s\theta_s\epsilon_s(1-\epsilon_m)\tau^2 I_{b\eta}(T_s)}{A_m\theta_m\epsilon_m\tau I_{b\eta}(T_m) + A_g\theta_g(1-\tau)I_{b\eta}(T_g)} \tag{6}$$

where A_s, A_m, and A_g are the area of the source, the area of the mirror, and the area of the glass seen by the detector, respectively; θ_s, θ_m, and θ_g are the solid angle of source emission, the solid angle of mirror emission, and the solid angle of glass emission, respectively; $I_{b\eta}(T_s)$, $I_{b\eta}(T_m)$, and $I_{b\eta}(T_g)$ are the intensities of blackbody radiation at sample temperature, mirror temperature, and glass temperature, respectively.

The source forms an image on the submerged mirror and, beyond the mirror, the source radiation goes through the same optical path as the sample emission. Both the source image and the sample emission form another image at field-stop I2. By adjusting

the field-stop I2, the image of the sample can be made the same size as the image of the source. Putting another iris I1 along the optical path after the submerged mirror can cut down the solid angle of the sample emission to the extent that it is the same as that of the source reflection. That is, we have $A_{si} = A_m = A_g$, and $\theta_{si} = \theta_m = \theta_g$, where the subscript i stands for source image on the submerged mirror. It is well known that the image has the same product of area and solid angle as the source due to the principle of conservation of energy. This implies that $A_s\theta_s = A_{si}\theta_{si} = A_m\theta_m = A_g\theta_g$. Substituting this equation into Eq. (6) yields

$$\frac{P_{\text{so}}}{P_{\text{sa}}} = \frac{\epsilon_s(1-\epsilon_m)\tau^2 I_{b\eta}(T_s)}{\epsilon_m \tau I_{b\eta}(T_m) + (1-\tau) I_{b\eta}(T_g)} \tag{7}$$

This indicates that the best ratio which can be achieved depends only on the emittance and the temperature of the source and sample. Assuming the source operates at 2,700°C and the mirror and sample are at 1,300°C, the emissive power of the source P_{so} is an order of magnitude higher than the emissive power of the sample P_{sa}.

TEST OF THE APPARATUS

Some low-temperature tests were performed to ensure the viability of the apparatus. They include the separation of multiple reflections and measurements of the absorption coefficient of distilled water. Each test will be described in detail in the following sections.

Separation of Multiple Reflections

Tests of separation of multiple reflections were carried out with each measurement. A He-Ne laser beam was used in place of the infrared beam from the FTIR, since the laser beam is much brighter and easier to trace. The infrared beam passed through a pinhole and formed a bright spot 15 cm from the pinhole. The laser beam was aligned by making the laser beam pass through the pinhole and hit the bright spot. Clear water was used as the test medium. The optical path was set to simulate the real situation. The laser beam is first reflected by the water surface. The first reflection is sent back to the pinhole by carefully adjusting the incident laser beam. This indicates that the laser beam is incident normal to the water surface. The laser beam then passes through the clear water and is reflected by the submerged mirror. It was found that multiple reflections occur, forming several bright dots several centimeters apart at a plane 12 in. above the mirror. Since the refractive index of molten glass is expected to be larger than that of clear water, the separation of multiple reflections for molten glass is known to be even greater.

Measurements of the Absorption Coefficient of Water

Tests of the experimental setup were conducted with distilled water at room temperature. The distilled water was heated prior to the experiment to eliminate tiny bubbles in the water. The measurement of the absorption coefficient of water is essentially the same as that of molten glass. The experimental procedure follows that described in the previous

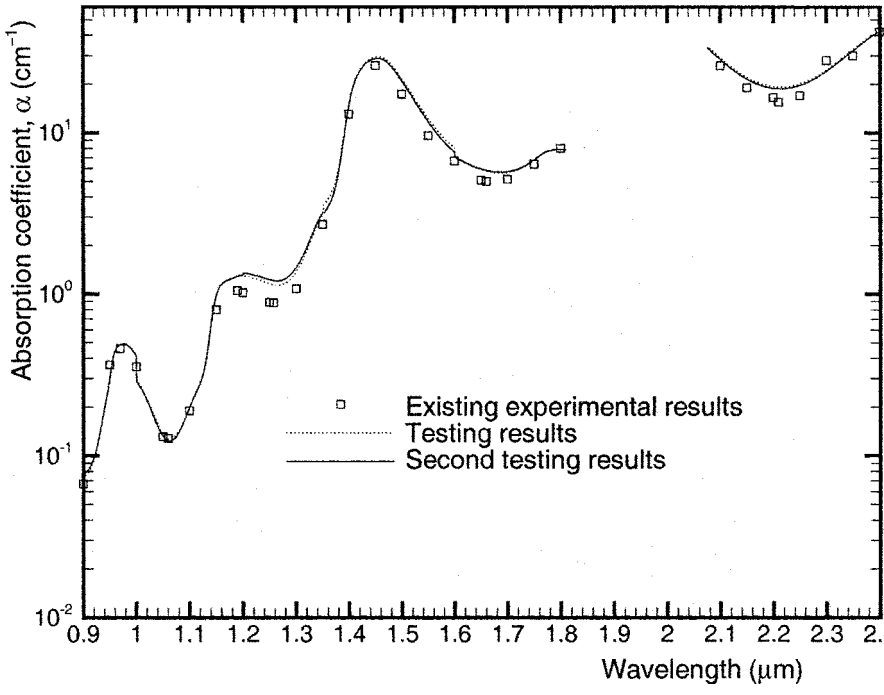

Figure 4. Absorption coefficient of distilled water measured with the current setup compared with published data [19, 20].

section. Both an MCT detector and a silicon detector were used to obtain high signal-to-noise ratio from 0.8 to 4.0 μm. The absorption coefficients obtained with different detectors overlap and coincide at 1.0 to 1.1 μm, indicating that the setup is independent of the detector used. The results are compared with previously published results [19, 20] and are shown in Figure 4. The two lines shown in the figure are two different measurements taken with the same setup. There are strong absorption bands between 1.8 and 2.1 μm and beyond 2.4 μm, with the absorption coefficient within one band exceeding the measurement capability of the current setup and, thus, no results are shown in this region. As is seen, the absorption coefficients measured with the current setup agree well with published data.

RESULTS AND DISCUSSION

Measurements were carried out for a number of glass samples, which were provided by Owens Corning. They belong to a category known as "E-glass," which is a family of calcia-alumina-silicate glasses with the chemical composition listed in Table 1. The signal was first collected with the platinum mirror roughly 5 mm beneath the glass surface. The glass layer thickness was reduced by 0.5 mm and the next signal was collected. This process was repeated until the platinum mirror was too close to the glass surface, at which point the surface tension of molten glass became significant. The surface tension of molten glass tends to warp the glass surface. The warped glass layer acts as a defocusing lens,

Table 1. Chemical composition of "E-glass" (from ASTM Standard D 578-99, Section 4.2.2).

SiO_2	CaO	Al_2O_3	B_2O_3	MgO
52–62 wt%	16–25 wt%	12–16 wt%	0–10 wt%	0–5 wt%
Na_2O	K_2O	TiO_2	F_2	Fe_2O_3
0–2 wt%	0–2 wt%	0–1.5 wt%	0.05–0.8 wt%	0–0.8 wt%

which leads to a decrease of signal. Decreasing the glass layer thickness by smaller steps was also attempted (e.g., 100 μm) to minimize the risk of warping the glass surface, which did not improve the signal. For each glass sample, measurements were conducted at five to six different glass layer thicknesses, to cover different ranges of absorption coefficient levels. Five sets of data were gathered at every thickness, and the average of the data was taken to minimize random uncertainty. The absorption coefficients were calculated with two average data taken at two different glass layer thicknesses. Since the data taken with the thinnest glass layer provide the largest signal, and thus the least random uncertainty, these data, together with the data taken at a different glass layer thickness, were used to calculate the absorption coefficients of the molten glass.

The temperature range of this experimental setup is limited by the thermophysical properties of glass and platinum. Since the glass samples start to soften sufficiently for the mirror to submerge into the glass pool at 1,200°C and the platinum rods have sufficient

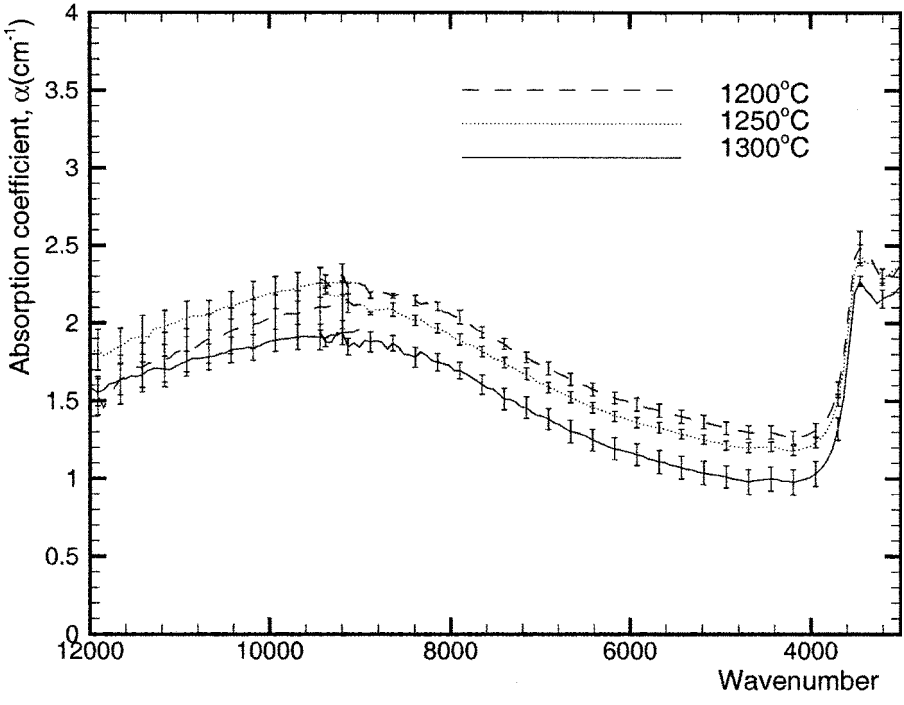

Figure 5. Absorption coefficient of glass sample no. 1.

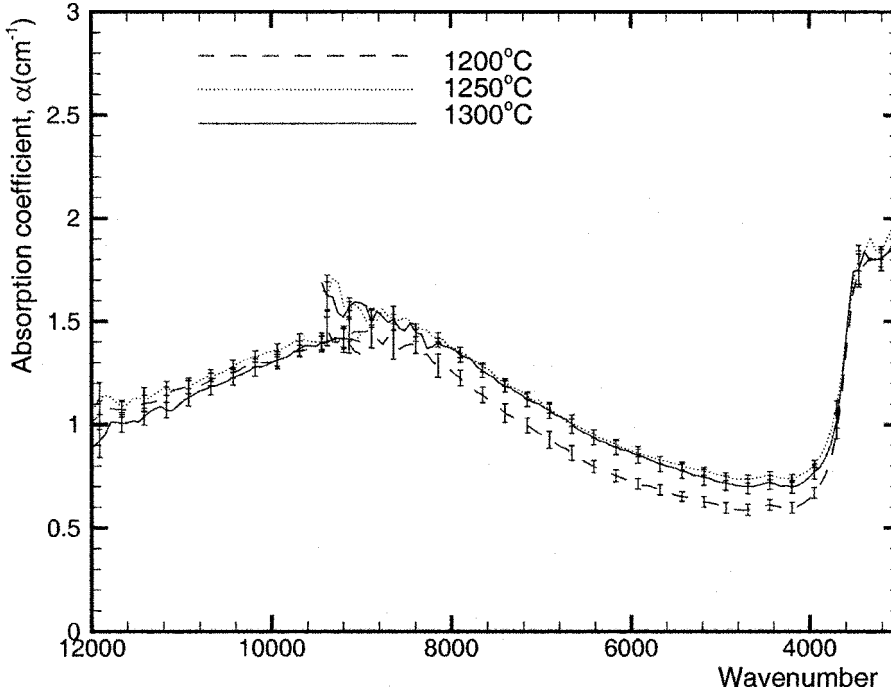

Figure 6. Absorption coefficient of glass sample no. 2.

rigidity at 1,300°C, this experimental setup has a temperature range of 1,200 to 1,300°C. The absorption coefficients of two typical samples are shown in Figures 5 and 6, for temperatures of 1,200, 1,250, and 1,300°C. The spectral absorption coefficients between 3,000 and 9,000 wavenumbers were measured with an MCT detector, and the spectral absorption coefficients between 9,000 and 11,000 wavenumbers were measured with a silicon detector. The absorption coefficients shown are the average value for the absorption coefficients calculated with data taken at different glass layer thicknesses. The standard deviations of the absorption coefficients are shown as error bars. The experimental results show that the absorption coefficients of molten glass are slightly temperature dependent. The absoprtion coefficients reach a local minima at approximately 4,000 wavenumbers, and increase sharply below 4,000 wavenumbers. The trends are in agreement with absorption coefficients of generic glass. The molten glasses show strong surface tension, which limits the the minimal achievable glass layer thickness to rougly 2 mm. Because the "submerged mirror" technique is a transmission technique, the relatively large glass layer thickness only permits the measurements of absorption coefficients of less than 3 cm^{-1} at such layer thickness.

CONCLUSIONS

An experimental method based on the "submerged mirror" technique has been presented. This method uses an FTIR spectrometer to measure the spectral intensity of

infrared light at different glass layer thicknesses. The multiple reflections of the infrared beam are separated, so that only the second reflection is collected. This ensures easy evaluation of the absorption coefficients from experimental data. Tests of the apparatus have been made with distilled water, for which the results agree well with existing data.

The absorption coefficients of molten glasses were measured at temperatures ranging from 1,200 to 1,300°C with both an MCT detector and a silicon detector. The absorption coefficients display a slight temperature dependence and uncertainties of less than 10%. Because the molten glasses have very strong surface tension, the minimal glass layer thickness that was achieved was roughly 2 mm. Since the "submerged mirror" technique is a transmission technique, this relatively large glass layer thickness limited the absorption coefficients measured to 3 cm^{-1} and below.

REFERENCES

1. Y. Shiraishi and K. Kusabiraki, Infrared Spectrum of High Temperature Melts by Means of Emission Spectroscopy, *High Temp. Sci.*, vol. 28, 1990.
2. W. B. Fussell and F. Stair, Preliminary Studies Toward the Determination of Spectral Absorption Coefficients of Homogeneous Dielectric Material in the Infrared at Elevated Temperatures, in S. Katzoff (ed.), *Symp. on Thermal Radiation of Solids*, NASA SP-55, pp. 287–292, 1965.
3. J. F. McClelland, Photoacoustic Spectroscopy, *Anal. Chem.*, vol. 55, pp. 89A–99A, 1965.
4. M. A. Havstad, W. McLean, and S. A. Self, Measurements of the Thermal Radiative Properties of Liquid Uranium, in *Proc. 27th Natl. Heat Transfer Conf.*, ASME, San Diego, CA, 1992.
5. E. D. Palik (ed.), *Handbook of Optical Constants of Solids*, Academic Press, New York, 1985.
6. R. K. Ahrenkiel, Modified Kramers-Kronig Analysis of Optical Spectra, *J. Opt. Soc. Am.*, vol. 61, no. 12, pp. 1651–1655, 1971.
7. M. Gottlieb, Optical Properties of Lithium Fluoride in the Infrared, *J. Opt. Soc. Am.*, vol. 50, no. 4, pp. 343–348, 1960.
8. J. R. Jasperse, A. Kahan, J. N. Plendl, and S. S. Mitra, Temperature Dependence of Infrared Dispersion in Ionic Crystals LiF and MgO, *Phys. Rev.*, vol. 140, no. 2, pp. 526–542, 1966.
9. J. Greenberg and L. J. Hallgren, *Rev. Sci. Instrum.*, vol. 31, no. 4, pp. 444–445, 1960.
10. J. D. Mackenzie, R. S. McDonald, and W. Murphy, Infrared Spectroscopy of Melts and Hygroscopic Glasses, *Rev. Sci. Instrum.*, vol. 32, no. 2, pp. 86–88, 1961.
11. W. Leupacher and A. Penzkofer, Refractive-Index Measurement of Absorbing Condensed Media, *Appl. Opt.*, vol. 23, pp. 1554–1558, 1984.
12. Y. Lu and A. Penzkofer, Optical Constants Measurements of Strongly Absorbing Media, *Appl. Opt.*, vol. 25, no. 1, pp. 221–225, 1986.
13. G. B. Varlamov, G. N. Vasil'chenko, V. I. Deshko, A. Y. Karavatskii, and O. E. Khlebnikov, Thermophysical and Optical Properties of Fluoride Crystals and Melts, *High Temp.–High Press.*, vol. 21, pp. 647–656, 1989.
14. J. L. Ebert and S. A. Self, The Optical Properties of Molten Coal Slag, in *Heat Transfer Phenomena in Radiation, Combustion and Fires*, Vol. HTD-106, pp. 123–126, ASME, New York, 1989.
15. S. B. Gupta and M. F. Modest, Measurement of Infrared Absorption Coefficient of Molten LiF and Li_2S, *28th Thermophysics Conf.*, Orlando, FL, Paper 93-2760, AIAA, 1993.
16. D. B. Tanner and R. P. McCall, Source of a Problem with Fourier Transform Spectroscopy, *Appl. Opt.*, vol. 23, pp. 2363–2368, 1984.
17. J. Ballard, J. J. Remedios, and H. K. Roscoe, The Effect of a Sample Emission on Measurements of Spectral Parameters Using a Fourier Transform Absorption Spectrometer, *J. Quantum Spectrosc. Radiat. Transfer*, vol. 48, pp. 733–741, 1992.

18. C. P. Tripp and R. A. McFarlane, Discussion of the Stray Light Rejection Efficiency of FT-IR Spectrometers: The Effects of Sample Emission on FT-IR Spectra, *Appl. Spectrosc.*, vol. 48, pp. 1138–1142, 1994.
19. W. M. Irvine and J. B. Pollack, Infrared Optical Properties of Water and Ice Spheres, *ICARUS*, vol. 8, pp. 324–360, 1968.
20. G. M. Hale and M. R. Query, Optical Constants of Water in the 200-nm to 200-μm Wavelength Region, *Appl. Opt.*, vol. 12, no. 3, pp. 555–563, 1973.